

# Electrochemical Investigation of Composite Cathodes with $\text{SmBa}_{0.5}\text{Sr}_{0.5}\text{Co}_2\text{O}_{5+\delta}$ Cathodes for Intermediate Temperature-Operating Solid Oxide Fuel Cell<sup>†</sup>

Jung Hyun Kim,<sup>‡</sup> Mark Cassidy,<sup>‡</sup> John T.S. Irvine,<sup>\*,‡</sup> and Joongmyeon Bae<sup>\*,§</sup>

<sup>‡</sup>School of Chemistry, University of St. Andrews, St. Andrews, Fife, KY16 9ST, United Kingdom, and

<sup>§</sup>Department of Mechanical Engineering, Korea Advanced Institute of Science and Technology, 373-1, Guseong-Dong, Yuseong-Gu, Daejeon, 305-701, Republic of Korea

Received June 21, 2009. Revised Manuscript Received October 29, 2009

The electrochemical characteristics of the samarium and strontium doped layered perovskite ( $\text{SmBa}_{1-x}\text{Sr}_x\text{Co}_2\text{O}_{5+\delta}$ ,  $x = 0.5$ ) have been investigated for possible application as a cathode material for an intermediate temperature-operating solid oxide fuel cell (IT-SOFC). The cathodic polarization of single-phase and composite cathodes with 10 mol % gadolinia-doped ceria ( $\text{Ce}_{0.9}\text{Gd}_{0.1}\text{O}_{2-\delta}$ , CGO91) shows that a weight ratio between  $\text{SmBa}_{0.5}\text{Sr}_{0.5}\text{Co}_2\text{O}_{5+\delta}$  (SBSCO) and CGO91 of 1:1 (50 wt % SBSCO and 50 wt % CGO91, SBSCO:50) gives the lowest area specific resistance (ASR) of  $0.10 \Omega \text{ cm}^2$  at  $600^\circ\text{C}$  and  $0.013 \Omega \text{ cm}^2$  at  $700^\circ\text{C}$ . The maximum and minimum electrical conductivity in SBSCO are  $1280 \text{ S cm}^{-1}$  at  $50^\circ\text{C}$  and  $280 \text{ S cm}^{-1}$  at  $900^\circ\text{C}$ , with the influence of oxygen partial pressure indicating p-type conduction. The maximum power density of SBSCO:50 in an anode supported SOFC was  $1.31 \text{ W cm}^{-2}$  at  $800^\circ\text{C}$  and  $0.75 \text{ W cm}^{-2}$  at  $700^\circ\text{C}$ .

## 1. Introduction

Materials based on layered perovskites have recently been the subject of increased interest as cathode materials for intermediate temperature-operating solid oxide fuel cells (IT-SOFC) working in the range of  $500\text{--}600^\circ\text{C}$  because the properties of high oxygen ion diffusivity and surface exchange coefficient were first identified during investigations of layered perovskites with respect to the colossal magneto resistance (CMR) phenomena.<sup>1–7</sup>

Layered perovskite oxide have the general formula  $\text{A}'\text{A}''\text{B}_2\text{O}_{5+\delta}$ , where  $\text{A}'$  can be lanthanides, or Y and  $\text{A}''$  can be Ba or Sr and the B site can be replaced with transition metal ions such as Co, Fe, and Mn.<sup>1–3</sup> In previous work, the layered perovskite with the chemical

composition of  $\text{YBaCo}_2\text{O}_5$  was first synthesized and investigated in 1993.<sup>8</sup> Notably, this material has a peculiar structure; oxygen vacancies in the Y layer are partially filled by oxygen and these oxygens are observed to be ordered. Significantly, the cation and anion ordering in  $\text{YBaCo}_2\text{O}_{5+\delta}$  can be controlled by various modifications and these phenomena show a number physical properties.<sup>9</sup>

For IT-SOFC cathode applications, the layered perovskite,  $\text{GdBaCo}_2\text{O}_{5+\delta}$  (GBCO), has recently been reported in the literature.<sup>3</sup> The area specific resistance (ASR) of this material on  $\text{Ce}_{0.8}\text{Gd}_{0.2}\text{O}_{2-\delta}$  (CGO82) electrolyte was reported as  $0.53 \Omega \text{ cm}^2$  at  $645^\circ\text{C}$  and this material was considered to be acceptable for application as cathode materials.<sup>3</sup> Tests were carried out on symmetrical half cells (GBCO/ $\text{Ce}_{0.9}\text{Gd}_{0.1}\text{O}_{2-\delta}$  (CGO91)/GBCO) giving good results of 0.065, 0.578, and  $3.874 \Omega \text{ cm}^2$  at 700, 600, and  $500^\circ\text{C}$  respectively.<sup>10</sup> Oxygen exchange studies of polycrystalline samples of the oxygen-deficient double perovskite  $\text{PrBaCo}_2\text{O}_{5+\delta}$  (PBCO) demonstrated that the oxygen kinetics in this cation-ordered structure type are significantly faster than in disordered perovskites.<sup>1</sup> Most importantly, ASR values of PBCO/gadolinia-doped ceria (CGO) composite cathodes on a CGO electrolyte were  $0.15 \Omega \text{ cm}^2$  at  $600^\circ\text{C}$  because of the rapid exchange kinetics.<sup>1</sup> Recent studies of  $\text{SmBaCo}_2\text{O}_{5+\delta}$  (SBCO) reported by Zhou, demonstrated a high performance at intermediate temperature ranges where the conductivity

<sup>†</sup> Accepted as part of the 2010 “Materials Chemistry of Energy Conversion Special Issue”.

\*John T. S. Irvine: jtsi@st-andrews.ac.uk, Tel: +44-1334-463817, Fax: +44-1334-463808 School of Chemistry, University of St. Andrews, St. Andrews, Fife, KY16 9ST, United Kingdom.

\*Joongmyeon Bae: jmbae@kaist.ac.kr, Tel: +82-42-350-3045, Fax: +82-42-350-8207 Department of Mechanical Engineering, Korea Advanced Institute of Science and Technology, 373-1, Guseong-Dong, Yuseong-Gu, Daejeon 305-701, Republic of Korea.

- (1) Kim, G.; Wnag, S.; Jacobson, A. J.; Reimus, L.; Brodersen, P.; Mims, C. A. *J. Mater. Chem.* **2007**, *17*, 2500.
- (2) Taskin, A. A.; Lavrov, A. N.; Ando, Y. *Appl. Phys. Lett.* **2005**, *86*, 091910.
- (3) Chang, A.; Skinner, S. J.; Kilner, J. A. *Solid State Ionics* **2006**, *177*, 2009.
- (4) Millange, F.; Caignaert, V.; Domengès, B.; Raveau, B.; Suard, E. *Chem. Mater.* **1998**, *10*, 1974.
- (5) Nakajima, T.; Kageyama, H.; Ueda, Y. *J. Phys. Chem. Solids* **2002**, *63*, 913.
- (6) Trukhanov, S. V.; Troyanchuk, I. O.; Hervieu, M.; Szymczak, H.; Barner, K. *Phys. Rev. B: Condens. Mater.* **2002**, *66*, 184424.
- (7) Akahoshi, D.; Uchida, M.; Tomioka, Y.; Arima, T.; Matsui, Y.; Tokura, Y. *Phys. Rev. Lett.* **2003**, *90*, 177203.

(8) Zhou, W. Z.; Liang, C.T. W.Y. *Adv. Mater.* **1993**, *5*, 735.

(9) Kwon, S. K.; Park, J. H.; Min, B. I. *Phys. Rev. B: Condens. Mater.* **2000**, *62*, 14637.

(10) Tarancón, A.; Peña-Martínez, J.; Marrero-López, D.; Morata, A.; Ruiz-Morales, J. C.; Núñez, P. *Solid State Ionics* **2008**, *179*, 2372.

of SBSCO is observed to vary from 815 to 434 S cm<sup>-1</sup> between 500 and 800 °C and the ASR on a Sm<sub>0.2</sub>Ce<sub>0.8</sub>O<sub>2</sub> (SDC) electrolyte being 0.51 and 0.19 Ω cm<sup>2</sup> at 650 and 700 °C, respectively. Power densities approaching to the 0.64 W cm<sup>-2</sup> at 800 °C were also observed.<sup>11</sup>

Ongoing IT-SOFC cathode research in our group shows Sr doped layered perovskite materials are promising cathode materials for use in IT-SOFC applications. For example, the effect of Sr substitution in YBaCo<sub>2</sub>O<sub>5+δ</sub> has been shown to decrease oxygen ordering within a single structural form.<sup>12</sup> At 50 mol % Sr-substitution (YBa<sub>0.5</sub>Sr<sub>0.5</sub>Co<sub>2</sub>O<sub>5+δ</sub>) electrical conductivity is seen to exhibit a maximum of 130 S cm<sup>-1</sup> at 150 °C with a value of 60 S cm<sup>-1</sup> at 700 °C. This compares to a maximum of 50 S cm<sup>-1</sup> at 300 °C and 20 S cm<sup>-1</sup> at 600 °C in the undoped material (YBaCo<sub>2</sub>O<sub>5+δ</sub>).<sup>8</sup> This suggests Sr substituted layered perovskite can be used as the potential cathode material for solid oxide fuel cell (SOFC). More recently, we have investigated the structural, thermal and electrochemical properties of SmBaCo<sub>2</sub>O<sub>5+δ</sub> (SBSCO)<sup>13</sup> and the electrochemical properties of members of the series LnBa<sub>0.5</sub>Sr<sub>0.5</sub>Co<sub>2</sub>O<sub>5+δ</sub> (Ln = Pr, Sm, and Gd) as cathode materials for IT-SOFC.<sup>14</sup> In this study, we have performed a more detailed investigation of the most promising members of this series, the Sm and Sr-doped system SmBa<sub>0.5</sub>Sr<sub>0.5</sub>Co<sub>2</sub>O<sub>5+δ</sub> (SBSCO) on Ce<sub>0.9</sub>Gd<sub>0.1</sub>O<sub>2-δ</sub> (CGO91) electrolyte. In this work a composite cathode SBSCO/CGO91 was used to optimize performance. The electrical conductivity and AC impedance of both single phase SBSCO and the SBSCO/CGO91 composite were measured in order to evaluate the potential for cathode application. The power density from these cathode systems on an anode supported 8YSZ electrolyte cell with CGO91 buffer layer was also determined at different temperatures.

## 2. Experimental Section

**2.1. Sample Preparation, X-ray Diffraction and Microstructure Analysis.** Samarium oxide (Sm<sub>2</sub>O<sub>3</sub>), barium carbonate (BaCO<sub>3</sub>), strontium carbonate (SrCO<sub>3</sub>), and cobalt oxide (Co<sub>3</sub>O<sub>4</sub>) were used for cathode synthesis. Stoichiometric amounts of these raw powders were mixed and ground in a mortar and pestle. These were then placed in a muffle furnace and calcined for 8 h at 1000 °C using various heating rates in order to decompose the carbonate. A further heat treatment of 36 h at 1100 °C was carried out after ball milling (bar type) for 24 h with acetone. The X-ray diffraction (XRD) patterns of the prepared samples were obtained in a Philips Diffractometer using Cu radiation (λ = 0.15418 nm). The data obtained were compared to reference data for the identification of crystal structures and phases.

The microstructures of symmetrical half cells were investigated using field emission scanning electron microscope (FE-SEM, S-4200, Hitachi) combined with energy-dispersive spectroscopy (EDS).

**Table 1. Chemical Compositions and Their Initials in This Research**

composition	initials
SmBa <sub>0.5</sub> Sr <sub>0.5</sub> Co <sub>2</sub> O <sub>5+δ</sub>	SBSCO
Ce <sub>0.9</sub> Gd <sub>0.1</sub> O <sub>2-δ</sub>	CGO91
90 wt % SBSCO and 10 wt % CGO91	SBSCO:10
80 wt % SBSCO and 20 wt % CGO91	SBSCO:20
70 wt % SBSCO and 30 wt % CGO91	SBSCO:30
60 wt % SBSCO and 40 wt % CGO91	SBSCO:40
50 wt % SBSCO and 50 wt % CGO91	SBSCO:50
40 wt % SBSCO and 60 wt % CGO91	SBSCO:60
30 wt % SBSCO and 70 wt % CGO91	SBSCO:70

**2.2. Electrochemical Characterization.** Ten mol % gadolinia-doped ceria (Ce<sub>0.9</sub>Gd<sub>0.1</sub>O<sub>2-δ</sub>, CGO91, Praxair Specialty Ceramics) was used for the electrolyte. Electrolyte pellets were prepared by pressing the powders at a pressure of 2 × 10<sup>3</sup> kg/m<sup>2</sup> and sintered at 1400 °C for 4 h. The final geometry of sintered electrolyte pellets was approximately 21 mm in diameter and 2 mm in thickness.

Single-phase cathode and composite cathodes with CGO91 were used for electrochemical measurements in a symmetrical half cell arrangement. The initials of these cathodes are summarized in Table 1. Suitable inks were made by mixing powders with an appropriate solvent and binder system, these were then applied to the electrolytes using screen printing to form the symmetrical half cells and sintered for 1 h at 1000 °C in order to form a porous electrode structure well bonded to the electrolyte. The final surface area of the symmetric cell was about 1.09 cm<sup>2</sup>.

The measurements of electrochemical properties and area specific resistances (ASRs) of the cathodes were performed at open circuit voltage as a function of temperature between 500 and 850 °C with the increment of 50 °C in air. AC impedance characteristics were measured with a Solatron 1260 frequency analyzer over a frequency range 0.01 Hz to 1 MHz and a voltage amplitude of 50 mV. The cathode polarization was determined from the differences between the low- and high-frequency intercept on the impedance curves and divided by 2.

For the electrical conductivity measurements pellets were pressed and sintered at 1100 °C for 12 h in air. A rectangular shaped bar (3 mm × 3 mm × 8.5 mm) was cut from the sintered pellet and polished. The conductivities were measured using a four-terminal DC arrangement in a custom jig with a Keithley 2400 Source Meter over a temperature range of 50 to 900 °C at a rate of 5 °C/min. To assess the effect of atmosphere, we controlled the oxygen partial pressure (pO<sub>2</sub>) using Ar gas and measured it with a zirconia-based oxygen sensor; conductivity was measured using a four-terminal arrangement.

**2.3. Single-Cell Fabrication and Single-Cell Test.** Eight mole percent yttria-stabilized zirconia (8YSZ) electrolyte anode supported cells were fabricated as previously reported.<sup>15</sup> These were made to 5 cm × 5 cm and were cut to 2.5 cm × 2.5 cm for single-cell performance testing. To prevent the formation of undesired phases between the cobalt-based perovskite materials and 8YSZ,<sup>16,17</sup> we fabricated a buffer layer using a CGO91 slurry applied by spin coating onto to the surface of the sintered electrolyte. The buffer layer was sintered at 1300 °C for 3 h. Single-phase and composite cathodes were printed by screen printing and heat-treated at 1000 °C for 1 h.

(11) Zhou, Q.; He, T.; Ji, Y. *J. Power Sources* **2008**, *185*, 754.

(12) Nakamura, J.; Karppinen, M.; Karen, P.; Linden, J.; Yamauchi, H. *Phys. Rev. B: Condens. Mater.* **2004**, *70*, 144104.

(13) Kim, J. H.; Kim, Y.; Connor, P. A.; Irvine, J. T. S.; Bae, J.; Zhou, W. *J. Power Sources* **2009**, *194*, 704.

(14) Kim, J. H.; Cassidy, M., C.; Irvine, J. T. S.; Bae, J. *J. Electrochem. Soc.* **2009**, *156*(6), B682.

(15) Bae, J.; Lim, S.; Jee, H.; Kim, J. H.; Yoo, Y. S.; Lee, T. *J. Power Sources* **2007**, *172*, 100.

(16) Bolech, M.; Cordfunke, E. H. P.; Van Genderen, A. C. G.; Van der Laan, R. R.; Janssen, F. J. G.; Van Miltenburg, J. C. *J. Phys. Chem. Solids* **1997**, *58*, 433.

(17) Kostoglou, G. Ch.; Ftikos, Ch. *J. Eur. Ceram. Soc.* **1998**, *18*, 1707.

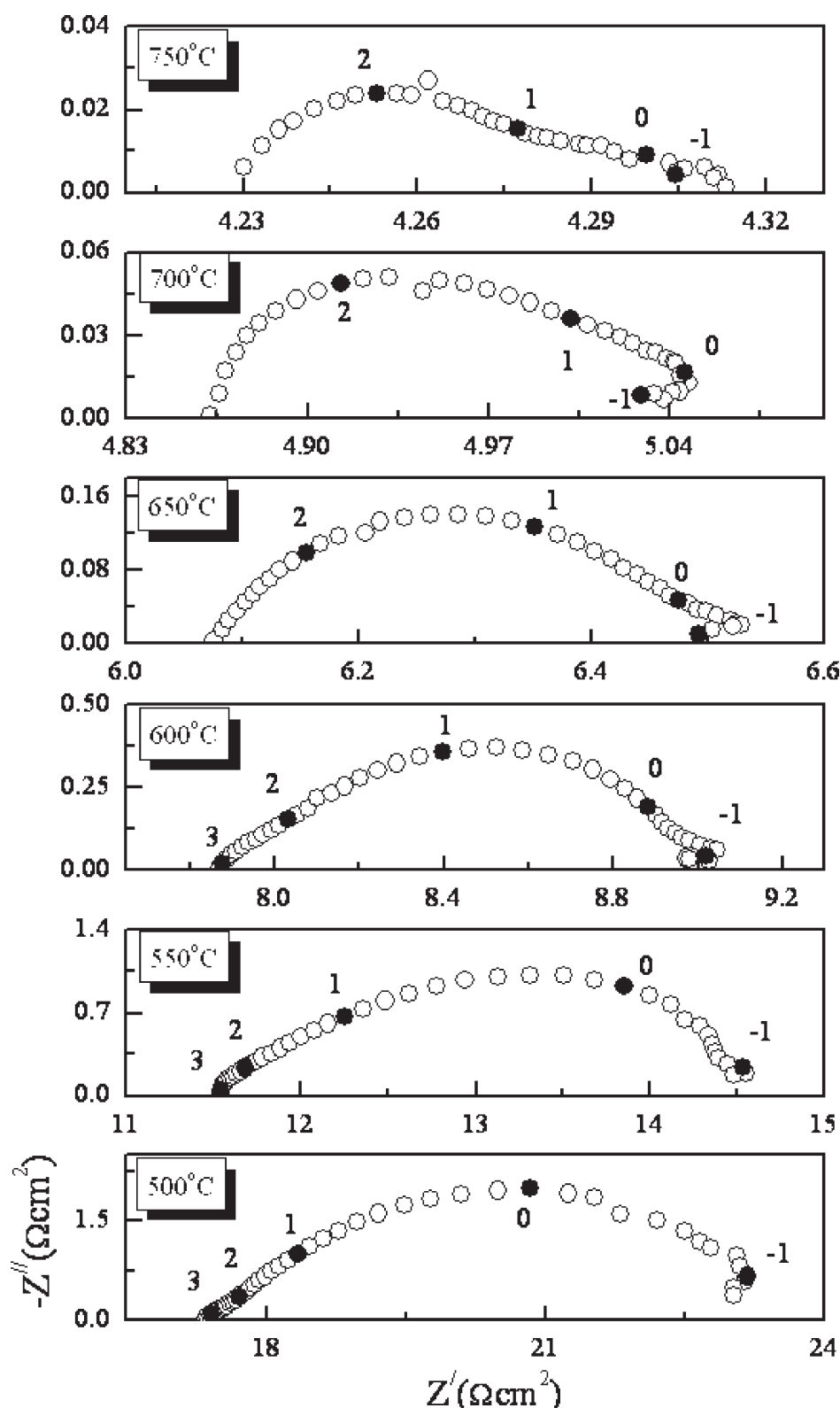


**Figure 1.** Impedance plots of SBSCO on CGO91 electrolyte from 500 to 750 °C. The numbers in these plots correspond to logarithm of frequency.

Voltage, current, and power characteristics were measured using Solatron 1286 using a 4 lead configuration. Three percent  $\text{H}_2\text{O}$  humidified  $\text{H}_2$  was supplied by bubbling through deionized water to the anode side at a flow rate of 100 sccm. Air was fed into cathode chamber as the oxidant gas. When supplying hydrogen gas and oxidant gas, mass flow controllers were used to control gas flow rates. Pt-paste and Pt-mesh were used for current collection.

### 3. Results

**3.1. Impedance Analysis of  $\text{SmBa}_{0.5}\text{Sr}_{0.5}\text{Co}_2\text{O}_{5+\delta}$  (SBSCO) on  $\text{Ce}_{0.9}\text{Gd}_{0.1}\text{O}_{2-\delta}$  (CGO91).** The impedance spectra of  $\text{SmBa}_{0.5}\text{Sr}_{0.5}\text{Co}_2\text{O}_{5+\delta}$  (SBSCO) on  $\text{Ce}_{0.9}\text{Gd}_{0.1}\text{O}_{2-\delta}$  (CGO91) electrolyte pellet, Figure 1, were collected to investigate the influence of temperature between 500

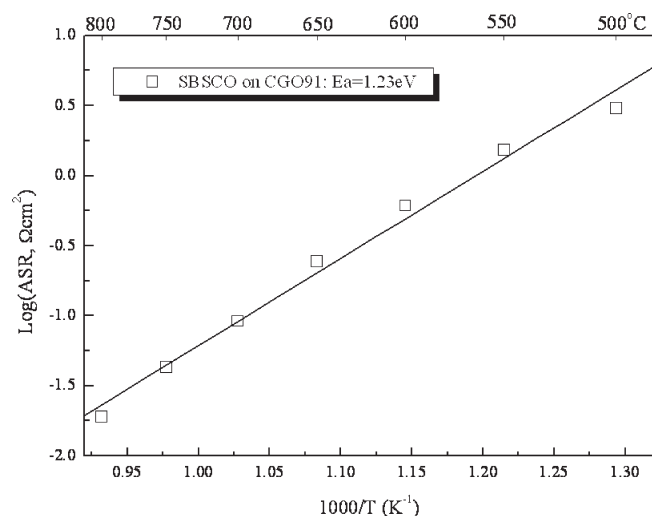


**Figure 2.** Area specific resistance (ASR) results of SBSCO with respect to the temperature.

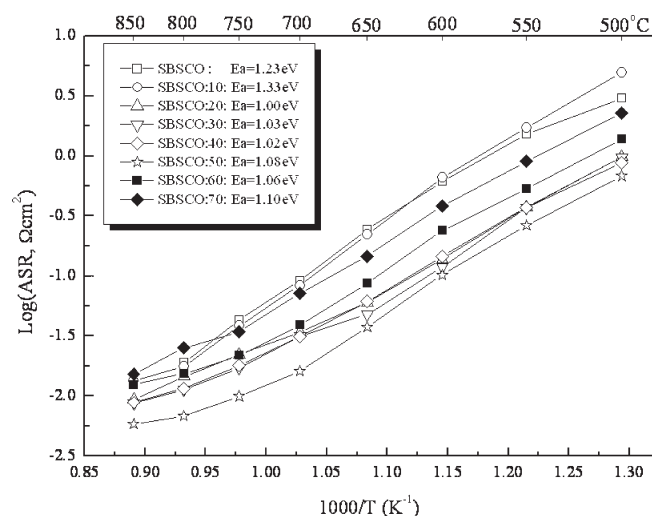


**Figure 3.** Area specific resistance results for various composite cathodes of CGO91 with SBSCO onto CGO91 electrolyte.

and 850 °C with an increment of 50 °C. Open circles are general impedance data points in symmetrical cells and closed black circles indicate decade of frequency. From these impedance spectra, the resolution of the separate arcs between middle ( $1 \times 10^3$  to  $1 \times 10^2$  Hz) and low frequency ( $10$  to  $1 \times 10^{-1}$  Hz) is clearer at lower temperatures (below 600 °C); however, the impedance response of high frequency consists of overlapped semicircles from 650 °C to high temperature. According to the impedance plots of mixed ionic and electronic conductor (MIEC) reported by Adler,<sup>18</sup> charge-transfer resistance originating from ion transfer at the interface of electrode and electrolyte is observed for the mid frequency arc. For the low-frequency arc, oxygen adsorption or dissociation on the cathode surface and diffusion through the electrode bulk are considered likely to be the main contributors. When comparing the results in this experiment with literature,<sup>18</sup> the dominant process in SBSCO may be associated with the charge transfer because the resistance caused by high-frequency range ( $1 \times 10^2$  Hz) is dominantly observed.

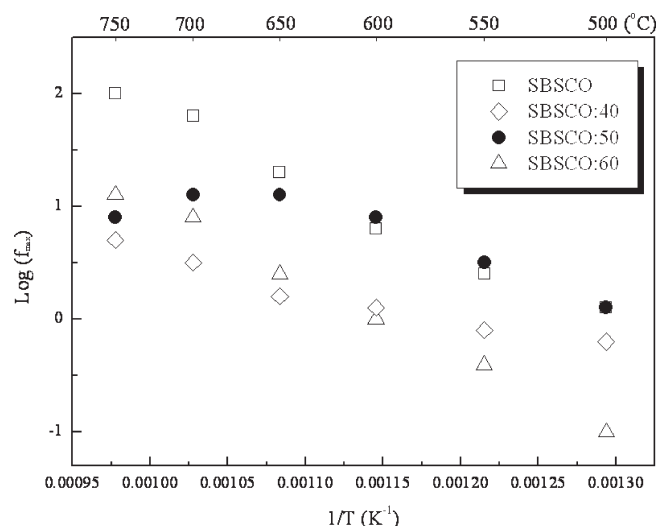


**Figure 4.** Relation between maximum frequencies of various cathodes and temperature.

**Table 2.** Fitting Results of SBSCO and Composite Cathodes with CGO91 at 700 °C<sup>a</sup>

compositions	$R_{ohm}$ ( $\Omega \text{ cm}^2$ )	$R_1$ ( $\Omega \text{ cm}^2$ )	$R_2$ ( $\Omega \text{ cm}^2$ )
SBSCO	4.845	0.1034	0.0916
SBSCO:20	7.790	0.0320	0.0423
SBSCO:30	6.770	0.0290	0.0312
SBSCO:50	3.383	0.0081	0.0192
SBSCO:70	3.13	0.0453	0.0961

<sup>a</sup> Total cathode polarization of the symmetrical cell has to be divided by 2. The component of inductor was on the order of  $1 \times 10^{-6}$  H from fitting results.

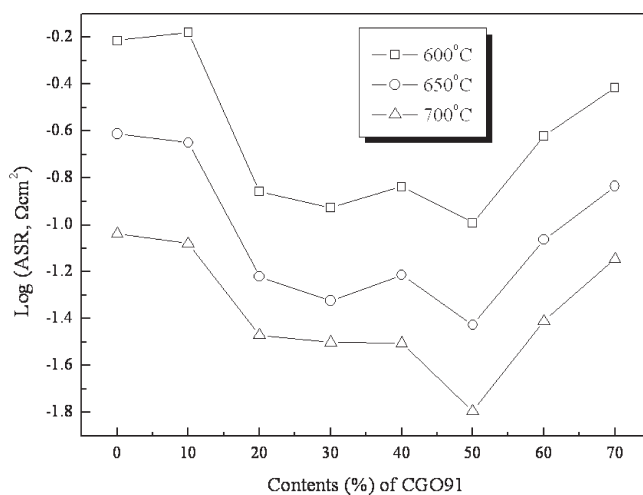


**Figure 5.** Dependence of cathodic polarization upon content of CGO91 at 600, 650, and 700 °C.

Arrhenius plots of the area specific resistances (ASRs) from impedance results of Figure 1 are shown in Figure 2. The ASR of SBSCO is observed about  $0.09 \Omega \text{ cm}^2$  at 700 °C and the activation energy of SBSCO with respect to temperature is 1.23 eV. Activation energies were calculated using eq 1

$$\log R_p = \log R_0 - \frac{E_a}{2.303RT} \quad (1)$$

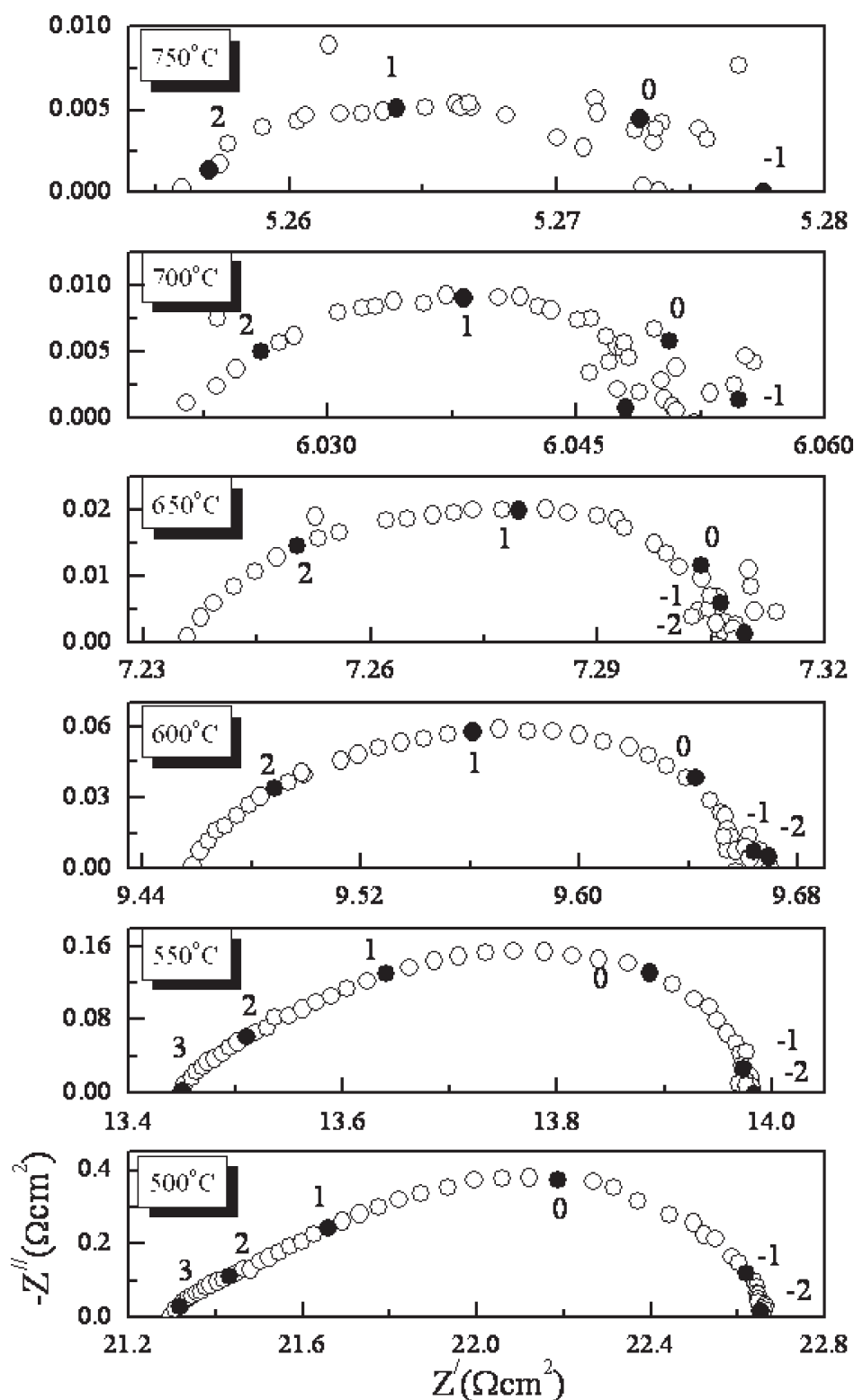


**Figure 6.** Impedance plots of SBSCO:50 at different temperatures.

where,  $R$  is a universal gas constant,  $T$  is absolute temperature, and  $R_0$  is related to the pre-exponential term in eq 1. Most usefully, the  $E_a$  in the exponential term is activation energy, which is directly related to the slope of Figure 2 and originates from all of the cathode

processes including oxygen adsorption, dissociation, bulk or surface diffusion, and the self-diffusion via electrolyte.<sup>19</sup> For comparison, the activation energy of  $\text{La}_{0.6}\text{Sr}_{0.4}\text{Co}_{0.2}\text{Fe}_{0.8}\text{O}_3$  (LSCF6428) was reported as 1.53 eV<sup>20</sup> and the value for SBSCO is significantly lower, indicating that the oxygen reduction processes in SBSCO are faster

(19) Barbucci, A.; Viviani, M.; Panizza, M.; Delucchi, M.; Cerisola, G. *J. Appl. Electrochem.* **2005**, *35*, 399.

(20) Dusastre, V.; Kilner, J. A. *Solid State Ionics* **1999**, *126*, 163.



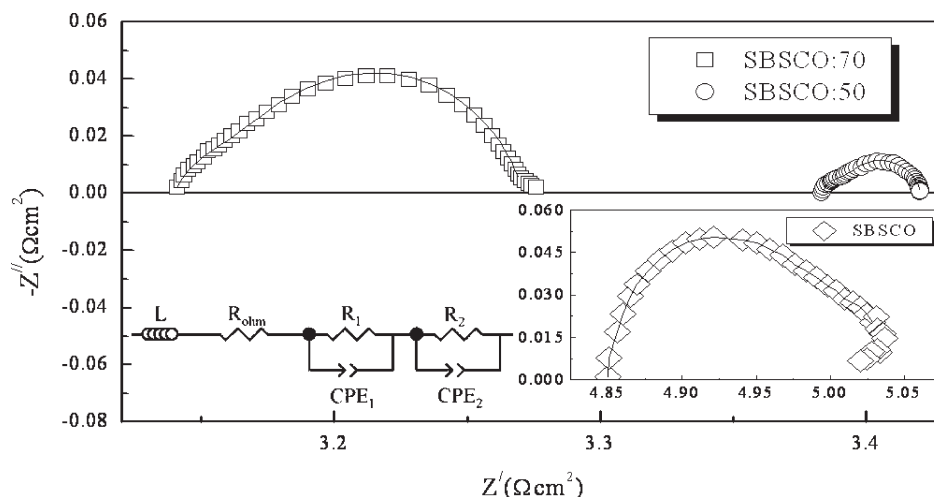


**Figure 7.** Impedance spectra of SBSCO, SBSCO:50 (50 wt % SBSCO and 50 wt % CGO91), and SBSCO:70 (30 wt % SBSCO and 70 wt % CGO91) at 700 °C. The points are from experimental results and the lines are from fitting results (shown as equivalent circuit in inset) with respect to the equivalent circuit.

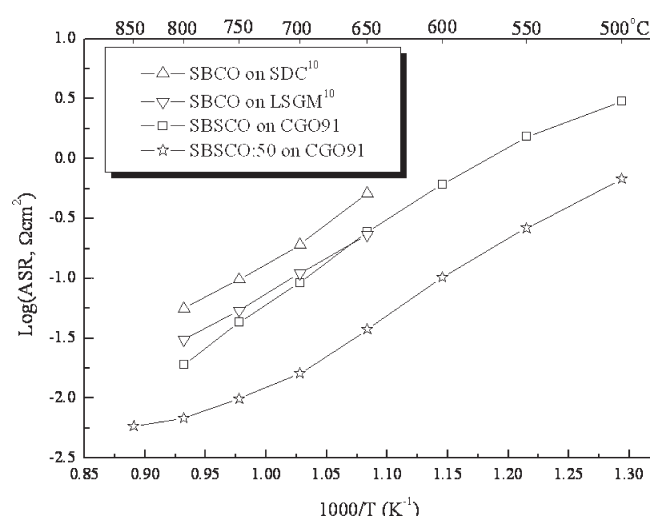


**Figure 8.** Comparison of ASR in SBSCO,<sup>10</sup> SBSCO, and SBSCO:50 as a function of temperature.

and have a lower temperature dependence than for LSCF6428.

Although the ASR and activation energy are low, the coefficient of thermal expansion (CTE) of SBSCO is still high (CTE,  $20\text{--}25 \times 10^{-6} \text{ K}^{-1}$  over 500 °C)<sup>14</sup> similar to other cobaltites ( $20\text{--}25 \times 10^{-6} \text{ K}^{-1}$ ).<sup>21</sup> This is significantly higher than common electrolyte materials ( $10.8 \times 10^{-6} \text{ K}^{-1}$  for YSZ,  $10.4 \times 10^{-6} \text{ K}^{-1}$  for LSGM and  $12.5 \times 10^{-6} \text{ K}^{-1}$  for CGO).<sup>22</sup> The significant CTE difference may be detrimental for the application of these types of materials in SOFC. In this work, composite cathodes were investigated, the ASRs of which are shown in Figure 3. Generally, the concept of composite cathode is used in order to maximize the triple phase boundary (TPB) between cathode and electrolyte to enhance performance.<sup>19</sup> However, a further effect is to reduce any mismatch in CTE between the electrolyte and cathode

material, which may permit the use of a materials where the CTE mismatch would be untenable in the single phase. In Figure 3, the abbreviation SBSCO:30, the numerical figure represents the 30 wt % CGO91 in the composite. The ASR of the SBSCO:50 composite was observed as 0.013 and 0.10  $\Omega \text{ cm}^2$  at 700 and 600 °C, respectively, and showed the best performance of the composite cathodes in this series. The enhanced cathode performance of SBSCO:50 was not only the effect of maximized composite cathode but also property of MIEC caused by various easy oxygen pathways as one of the properties in layered perovskite.<sup>1</sup> A change of slope at about 700 °C was observed in Figure 3. The slope change occurs at the composition of SBSCO:50. However, it was not observed in the other compositions. This phenomenon is related with the oxygen reduction reaction mechanism.<sup>23</sup> It can be also observed in Figure 4. Figure 4 displays the relation between maximum frequencies of various cathodes tested and temperature. From these results, the frequency magnitude from the samples except for SBSCO:50 shows linear behavior as a function of temperature. However, a transition for SBSCO:50 is observed near 650 °C. Accordingly, a different oxygen reduction reaction is directly related with SBSCO:50. Significantly, the ASR value of SBSCO:50 was lower than LSCF6428 reported by Steele and Bae.<sup>24</sup> As mentioned above, the activation energy of SBSCO was 1.23 eV in Figure 2. The composite cathodes, for example, from SBSCO:20 to SBSCO:70, show activation value decreasing to 1.00 eV because of the extension of chemically active sites as the TPB expands giving an enhanced oxygen reduction process in the composite cathode.

The ASR values for the composite cathodes at 600, 650, and 700 °C, respectively are shown in Figure 5. These show strong dependence relative contents of CGO91 and SBSCO, with the lowest ASR value being observed from

(21) Wei, B.; Lü, Z.; Li, S.; Li, Y.; Liu, K.; Su, W. *Electrochem. Solid-State Lett.* **2005**, *8*, A428.

(22) Minh, N. Q.; Takahashi, T. *Science and Technology of Ceramic Fuel Cell*; Elsevier: New York, 1995.

(23) Baque, L.; Caneiro, A.; Moreno, Mario S.; Serquis, A. *Electrochem. Commun.* **2008**, *10*, 1905.

(24) Steele, B. C. H.; Bae, J. M. *Solid State Ionics* **1998**, *106*, 255.

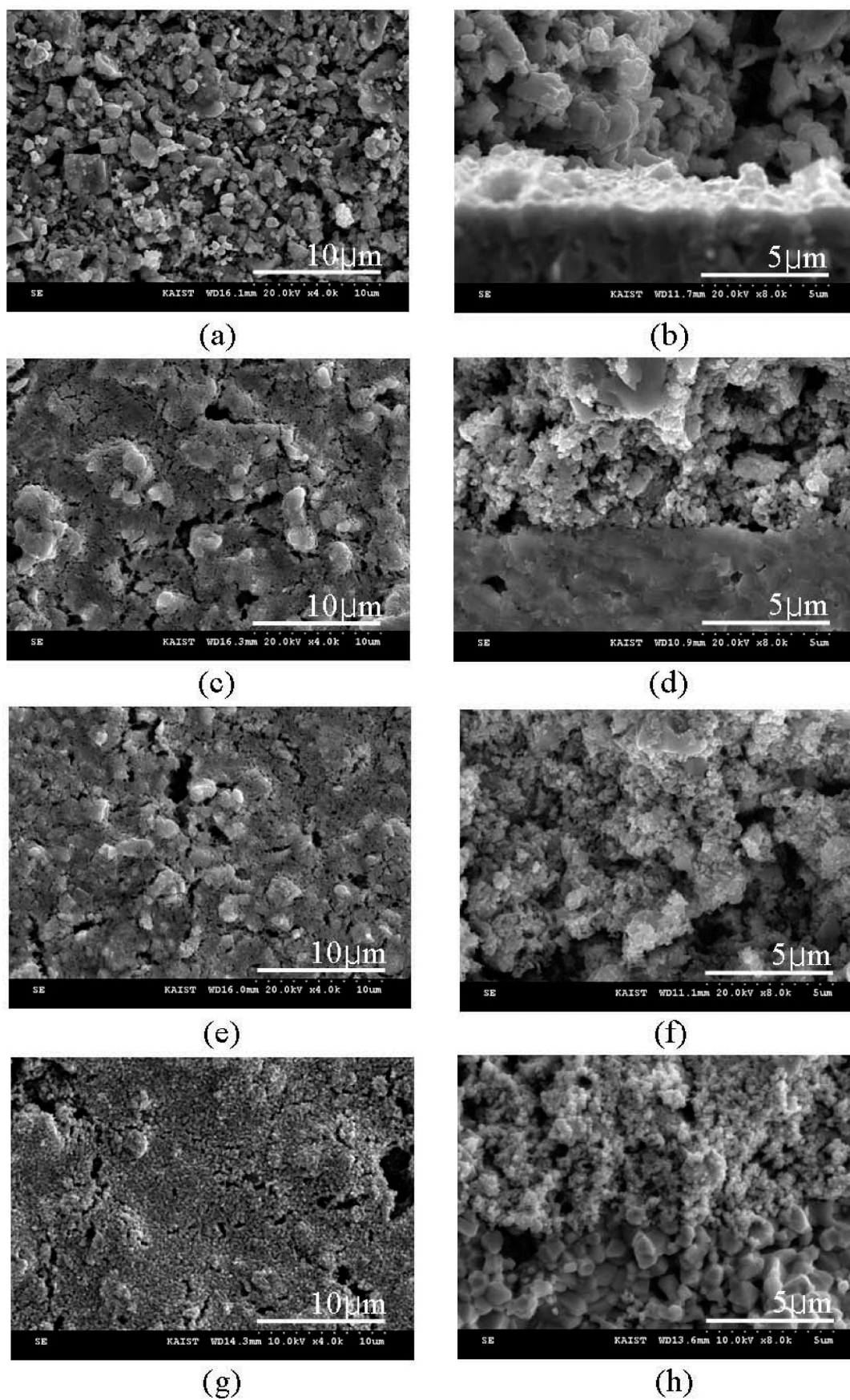


**Figure 9.** Scanning electron microscope (SEM) images of SBSCO, SBSCO:40, SBSCO:50, and SBSCO:70 after sintering. (a, c, e, g) Top-view images of SBSCO, SBSCO:40, SBSCO:50, and SBSCO:70; (b, d, f, h) cross-section images of SBSCO, SBSCO:40, SBSCO:50, and SBSCO:70.

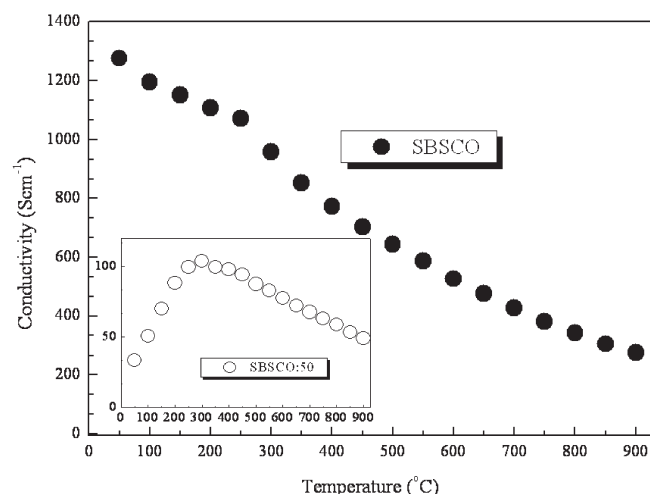


**Figure 10.** Electrical conductivity of SBSCO, SBSCO:50 with respect to the temperature.

the specimen of SBSCO:50 as discussed before. At values greater than 50 wt % of CGO91 in SBSCO, the ASR increases as it is related to the effective percolation of electrically conducting phase present.<sup>19</sup> ASR can also be seemed to rise significantly at lower CGO91 levels as below 10 wt %, there is significant detrimental effect due to reduced triple phase boundary.

Figure 6 shows the impedance plots of SBSCO:50 with temperature. When comparing the arcs of SBSCO (Figure 1) with SBSCO:50 (Figure 6), the arc behavior of SBSCO in the vicinity of high frequency ranges ( $1 \times 10^3$  to  $1 \times 10^2$  Hz) changes with respect to the temperature. However, the impedance plots of SBSCO:50 in Figure 6 show similar behavior they are dominated by composite effects.

The impedance spectra and fitting results of SBSCO, SBSCO:50, and SBSCO:70 are displayed in Figure 7. For comparative analysis of single phase and composite cathodes the ohmic resistance of the symmetrical cell and cathode polarization were obtained by fitting the impedance spectroscopy results to an equivalent circuit shown in the inset of Figure 7. This comprised of an inductor, series resistance and two distributed elements each consisting of a resistor and constant phase element (CPE) in parallel with the distributed elements representing the mid and low frequency arcs. In this equivalent circuit, the resistance from the middle frequency (MF) is as attributed to the charge transfer ( $R_1$ ), and the lower frequency (LF) arc to the oxygen dissociation and bulk or surface oxygen diffusion process ( $R_2$ ). The component results from equivalent circuit analysis at 700 °C are summarized in Table 2 and show that  $R_1$  is higher than  $R_2$  in the single-phase cathode, suggesting that charge-transfer resistance was considered as the rate-determining step (RDS) in single-phase cathode at 700 °C. However, the  $R_2$  values were higher than that of  $R_1$  in the composite cathode system. This implies that the cathodic polarization of the composite cathode was governed by  $R_2$  at 700 °C. According to Figure 7 and Table 2, the ohmic resistance trend follows the contents of CGO91 in the

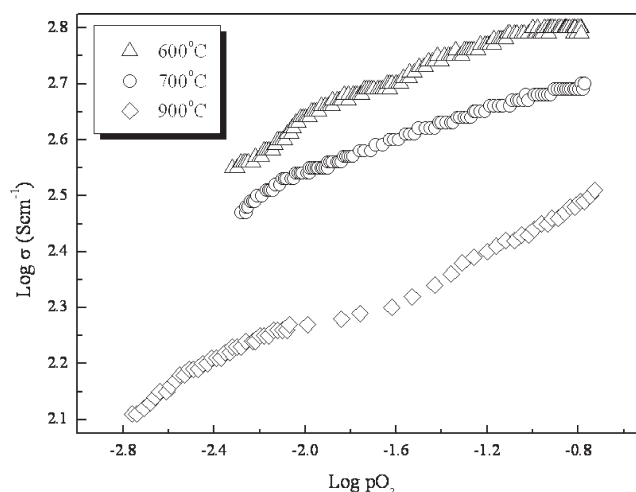


**Figure 11.** Electrical conductivities of SBSCO with  $pO_2$  at 600, 700, and 900 °C.

SBSCO composite with the ohmic resistance of SBSCO:CGO91 decreasing with increasing content of CGO91 because the thickness of composite cathodes was reduced when higher contents of CGO91 were included in the composite cathode. These results are consistent with those from composite cathodes comprising LSCF and CGO.<sup>25</sup>

The ASR differences between  $SmBaCo_2O_{5+\delta}$  (SBSCO),<sup>11</sup> SBSCO, and SBSCO:50 are summarized in Figure 8. At 700 °C the Sr substituted SBSCO and the SBSCO:50 achieve much smaller ASR values of  $0.092 \Omega cm^2$  and  $0.013 \Omega cm^2$  respectively than the non Sr substituted material ( $0.19 \Omega cm^2$ ).<sup>11</sup> Comparison to other composite cathode systems such as 50:50 mixtures of  $PrBaCo_2O_{5+\delta}$  (PBCO) and CGO (PBCO:50),<sup>1</sup> shows that at 600 °C the ASR values of SBSCO:50 ( $0.10 \Omega cm^2$ ) were lower than those of PBCO:50 ( $0.15 \Omega cm^2$ ).<sup>1</sup> At this time it is believed that SBSCO:50 shows the lowest ASR value reported for a layered perovskite oxide system.<sup>1,3,11</sup>

The microstructures of the various compositions are shown in Figure 9. The surface microstructure of a SBSCO single-phase cathode (Figure 9a) comprises multisized SBSCO particles. However, the surface morphology of composite cathodes showed different characteristics and the compact structures of SBSCO and CGO91 were found in Figure 9c, e, and g. The open porous structure in the SBSCO cathode correlates well with the observed AC impedance behavior, with the rate-determining step being dominated by the availability of TPB for charge transfer as opposed to relatively large availability of particle surface for surface adsorption and diffusion of oxygen species. However, the structure of composite cathodes reveals a larger SBSCO grain and smaller CGO91 grain this increases the amount of contact between SBSCO and CGO91 (Figure 9d, f, and h) resulting in increased TPB length. This changes the rate determining step to the surface adsorption and diffusion effects as there is now sufficient TPB for efficient charge transfer

(25) Perry Murray, E.; Sever, M. J.; Barnett, S. A. *Solid State Ionics* **2002**, 148, 27.



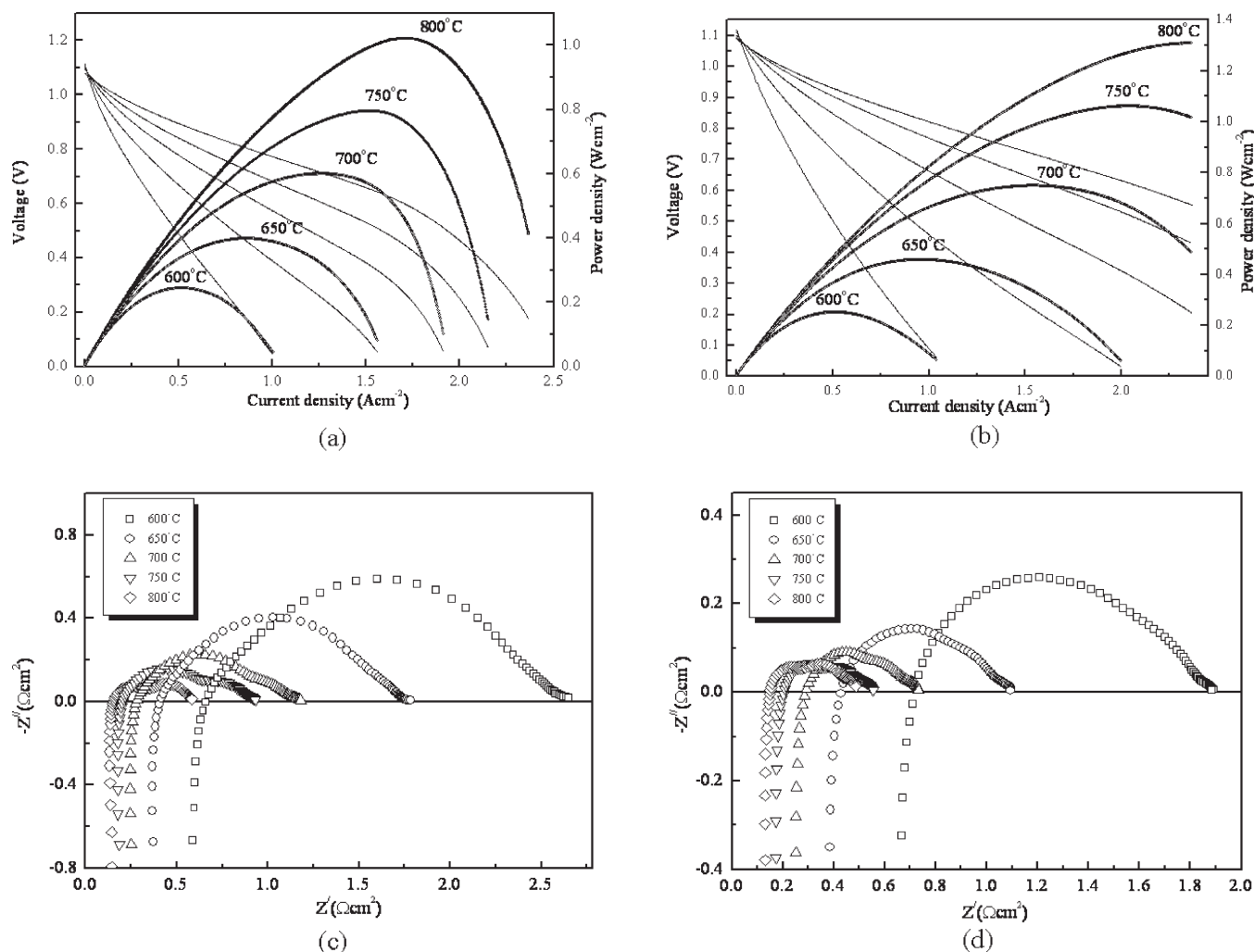


**Figure 12.** (a)  $I$ – $V$  polarization curves for Ni-8YSZ supported thin 8YSZ electrolyte and CGO91 buffer layer with SBSCO at different temperatures, (b)  $I$ – $V$  polarization curves for Ni-8YSZ supported thin 8YSZ electrolyte and CGO91 buffer layer with SBSCO:50 at different temperatures, (c) impedance spectra of Ni-8YSZ supported thin 8YSZ electrolyte and CGO91 buffer layer with SBSCO at different temperatures, and (d) impedance spectra of Ni-8YSZ supported thin 8YSZ electrolyte and CGO91 buffer layer with SBSCO:50 at different temperatures.

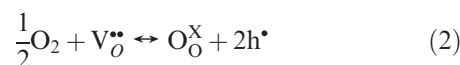
with the main resistive component now being  $R_2$ , consistent with the low ASR values exhibited by these composites in Figures 3 and 5.

### 3.2. Electrical Conductivity of SBSCO and SBSCO:50.

The variation in electrical conductivity of SBSCO with respect to temperature is summarized in Figure 10. The maximum and minimum conductivities in this material are  $1280 \text{ S cm}^{-1}$  at  $50^\circ\text{C}$  and  $280 \text{ S cm}^{-1}$  at  $900^\circ\text{C}$  and are metallic in nature. This metallic nature is characteristic of Co-based perovskite oxides and is due to the energy band overlap between Co-3d and O-2p.<sup>26</sup> Hole conduction in cobaltites, including metallic conduction, comes from the presence of  $\text{Co}^{4+}$  ions and thermally generated charge disproportionation where  $2\text{Co}^{3+}$  changes to  $\text{Co}^{2+}$  and  $\text{Co}^{4+}$ . The inset of Figure 10 shows the conductivity of the composite SBSCO:50 with respect to temperature. The overall electrical conductivity of SBSCO:50 is much lower than that of SBSCO because of the composite nature of this material and it shows semiconducting behavior below  $300^\circ\text{C}$ . Above

this temperature, there is a transition to a metallic behavior with the maximum being around  $105 \text{ S cm}^{-1}$ .

The electrical conductivity of SBSCO with respect to the oxygen partial pressure ( $p\text{O}_2$ ) is shown in Figure 11. From these results, electrical conductivity decreased with increasing temperature and increased with increasing  $p\text{O}_2$ . This indicates that the conductivity of SBSCO shows a metallic p-type behavior. From these results, the slope of  $\log(\sigma)$  versus  $1000/T \text{ (K}^{-1}\text{)}$  in SBSCO at 600 and  $700^\circ\text{C}$  was found to be  $1/6$  and  $1/4$ – $1/5$  at  $900^\circ\text{C}$ . The carriers in SBSCO are thus thought to be created by following eq 2.



**3.3. Single-Cell Performance of Anode-Supported Solid Oxide Fuel Cell with SBSCO and SBSCO:50.** The performance of anode-supported cells using SBSCO and SBSCO:50 cathodes are illustrated in Figure 12 (a) and (b) with values for open circuit voltages summarized in Table 3. The OCVs are close to the values of Nernst potential expected when using humidified hydrogen (3%  $\text{H}_2\text{O}$ ) as a fuel and demonstrate the cells are well-sealed

(26) Moon, J. W.; Masuda, Y.; Seo, W. S.; Koumoto, K. *Mater. Sci. Eng.* **2001**, *B85*, 70.

**Table 3. Summarized OCVs of SBSCO and SBSCO:50 at 800, 750, 700, 650, and 600 °C**

compositions	OCVs (V)				
	T (°C)				
	600	650	700	750	800
SBSCO	1.114	1.104	1.097	1.093	1.079
SBSCO:50	1.118	1.109	1.100	1.092	1.087

with gastight electrolytes.<sup>21</sup> The maximum power densities for the single-phase cathodes (Figure 12a) were  $0.24 \text{ W cm}^{-2}$  at 600 °C,  $0.60 \text{ W cm}^{-2}$  at 700 °C, and  $1.02 \text{ W cm}^{-2}$  at 800 °C. By comparison, the maximum power densities for SBSCO:50-based cells were as high as  $0.25 \text{ W cm}^{-2}$  at 600 °C,  $0.75 \text{ W cm}^{-2}$  at 700 °C and  $1.31 \text{ W cm}^{-2}$  at 800 °C (Figure 12b). Similar composite systems such as  $\text{GdBa}_{1-x}\text{Sr}_x\text{Co}_2\text{O}_{5+\delta}$  (GBSCO) (having same crystalline structure ( $x = 0.6$ ) of SBSCO) on  $\text{La}_{0.8}\text{Sr}_{0.2}\text{Ga}_{0.8}\text{Mg}_{0.2}\text{O}_{2.8}$  (LSGM) electrolyte exhibited power densities of  $0.25 \text{ W/cm}^2$  at 700 °C. Through a different electrolyte was used in this experiment, the power density of SBSCO:50 is twice that of the composite cathode with GBSCO.<sup>27</sup> The impedance spectra of single cells measured under open circuit conditions are shown in Figure 12c and d, with Figure 12c showing the response of the single-phase cathode and Figure 12d that of the composite. The polarization resistance of the cell was taken as the difference between high- and low-frequency intercepts on the  $x$  axis. In this arrangement, the AC impedance represents the total resistance of the cell comprising both anode and cathode responses, which were not possible to separate in this set up. However, as the anode support was nominally the same across all of the cells, it is assumed that any significant differences in performance are due to the differences in cathode composition and microstructure. From Figure 12d, the polar-

ization resistances of the composite cathode were observed as 1.49, 1.02, 0.82, 0.70, and  $0.55 \text{ } \Omega \text{ cm}^2$  at 600, 650, 700, 750, and 800 °C, respectively. These are lower than the SBSCO single-phase cathode cell, are in line with the previously presented component data, and reinforce the advantages of a composite cathode system to attain maximum cell performance in this system.

#### 4. Conclusion

The electrochemical properties of  $\text{SmBa}_{0.5}\text{Sr}_{0.5}\text{Co}_2\text{O}_{5+\delta}$  (SBSCO) and  $\text{Ce}_{0.9}\text{Gd}_{0.1}\text{O}_{2-\delta}$  (CGO91) composite cathodes are reported and these materials considered for cathode application of intermediate temperature-operating solid oxide fuel cells (IT-SOFC). Single-phase SBSCO exhibited metallic behavior with electrical conductivities of  $1280 \text{ S cm}^{-1}$  at 50 °C and  $280 \text{ S cm}^{-1}$  at 900 °C. The best electrochemical performance both in symmetrical half cells and anode supported cells was seen in the specimens that comprised a composite of 50 wt % SBSCO and 50 wt % of CGO91 (SBSCO:50). This composite exhibited half cell ASRs of 0.10 and  $0.013 \text{ } \Omega \text{ cm}^2$  at 600 and 700 °C, respectively, and cell power densities of  $1.06 \text{ W cm}^{-2}$  at 750 °C,  $0.75 \text{ W cm}^{-2}$  at 700 °C, and  $0.46 \text{ W cm}^{-2}$  at 650 °C. All of these results suggest that the SBSCO and CGO91 composite is a highly promising cathode material for IT-SOFC applications.

**Acknowledgment.** This work is generated from the projects within the Core Technologies for Fuel Cells (CTFC) development program, which is supported by the Ministry of Knowledge Economy (MKE), the Brain Korea 21 (BK21) program of the Ministry of Education and Science Technology (MEST), and the 5 kWe Diesel-driven SOFC system with the Korean Electric Power Research Institute (KEPRI) from the Republic of Korea. Additionally, we thank the Engineering and Physical Sciences Research Council (EPSRC) and Carbon Trust of the United Kingdom for Senior Fellowship, Carbon Vision and Platform Grant support.

(27) Kim, J.-H.; Prado, F.; Manthiram, A. *J. Electrochem. Soc.* **2008**, *155*(10), B1023.